Influence of charge-density-wave structure on paramagnetic spin waves in alkali metals

Yong Gyoo Hwang and A. W. Overhauser

Department of Physics, Purdue University, West Lafayette, Indiana 47907

(Received 8 January 1988)

A spin-wave theory is developed for alkali metals having a charge-density-wave (CDW) structure. For simplicity the spin-dependent part of the many-body interaction between quasiparticles is taken as a constant, thereby neglecting Landau parameters B_n with $n \geq 1$. In a CDW state the velocity distribution is not only anisotropic, but open-orbit motion becomes possible. As a result, the motion of an electron is significantly modified. Since the known properties of alkali metals indicate charge-density-wave structure, the interpretation of experimental spin-wave data is reconsidered. The revised values of the Landau parameter B_0 and the fraction of electrons in open orbits η for potassium are found to be $B_0 = -0.252(\pm 0.003)$ and $\eta = 0.048(\pm 0.015)$ when only the open-orbit effect is included. $B_0 = -0.221(\pm 0.002)$ and $\eta = 0.042(\pm 0.013)$ if Fermi surface distortion is also included. It is also shown that observed splittings of spin-wave side bands can be explained when the effects of the CDW domain structure are recognized.

I. INTRODUCTION

Since conduction-electron spin resonance (CESR) was first observed in 1952,[1] extensive work has been done to yield valuable information on the spin-dependent part of the many-body interaction. As was first noticed by Dyson,[2] CESR becomes possible from the fact that an electron returns many times to the rf skin layer where the external oscillating magnetic field is applied, before it diffuses further into the sample. A theory of CESR was developed by Dyson[2] for a noninteracting electron gas in a static magnetic field normal to the surface, and later extended for an arbitrary angle by Lampe and Platzman.[3] When the many-body interaction is taken into account in the framework of Landau Fermi-liquid theory, it was shown by Silin[4] that an interacting Fermi system in a static magnetic field can have collective excitations with nonzero wave number analogous to spin waves in ferromagnetic materials. A transmission-electron spin resonance (TESR) experiment[5] is one the most powerful tools in investigating the many-body interaction in a Fermi system, since the existence of spin waves exclusively depends on the presence of the many-body interaction. Theories of paramagnetic spin waves have been developed by Platzman and Wolff[5] (PW) and others.[6,7] In those theories, it has been assumed that the electron energy spectrum is free-electron-like and that the Fermi surface is very close to a perfect sphere. But there is a large amount of experimental data which cannot be explained by free-electron-like theories.[8] TESR data in particular show several anomalous features which have not been interpreted by conventional theories. The main CESR sometimes shows a splitting of about 0.5 G.[9] This phenomenon was explained quantitatively as the result of an anisotropic g factor in the CDW state by Overhauser and de Graaf.[10] Spin-wave side bands sometimes show splittings into two or more components.[11]

In this study, an extension of the PW theory has been made to incorporate several charge-density-wave (CDW) effects: distortion of the Fermi surface, the presence of open-orbit motion, and domain structure. It is also shown that several anomalous experimental observations can be explained using this theory. In Sec. II relevant aspects of the CDW theory are reviewed. In Sec. III essentials of the Landau Fermi-liquid theory are recalled. In Sec. IV a simplified model is developed to incorporate CDW effects, and transmission of rf signals through a finite slab is obtained. In Secs. V the Platzman-Wolff theory, its CDW modifications, and experimental data for potassium are compared. In Sec. VI our results are summarized.

II. BRIEF REVIEW OF CHARGE-DENSITY-WAVE THEORY

It has been shown by Overhauser[12] that an interacting electron gas always suffers a spin-density-wave (SDW) or a charge-density-wave instability in the Hartree-Fock approximation, and that when correlation effects are taken into account the CDW instability is enhanced while the SDW instability is reduced. Alkali metals have very weak elastic stiffness[13,14] and very small Born-Mayer ion-ion repulsion;[15] they are expected to suffer (CDW) instabilities. Many otherwise anomalous data have been successfully explained by CDW theory.[8] Recently neutron diffraction satellites were observed,[16] so the direction and magnitude of **Q** are directly determined for potassium.

CDW structure can be described by including an extra sinusoidally varying potential with wave vector **Q** in addition to the usual crystal potential:

$$U^{\text{CDW}} = G \cos(\mathbf{Q} \cdot \mathbf{r}) , \tag{2.1}$$

where **Q** is the CDW wave vector and G is the periodic part of the exchange and correlation interaction. This periodic potential is sustained self-consistently by the resulting modulation of electron charge density $\rho(\mathbf{r})$:

$$\rho(\mathbf{r}) = \rho_0 [1 - p \cos(\mathbf{Q} \cdot \mathbf{r}')] , \tag{2.2}$$

where p is the fractional amplitude of the CDW. The Hartree potential of the electron charge density is neutralized by deformation of the positive-ion background. The one-electron Schrödinger equation can be approximated by

$$\left[\frac{p^2}{2m} + G \cos(\mathbf{Q} \cdot \mathbf{r}) \right] \Psi_k = \varepsilon_k^0 \Psi_k . \tag{2.3}$$

Self-consistency between the CDW potential and the charge modulation requires one to solve an integral equation for $G(\mathbf{k})$.[12] Since this is a very complicated problem, G will be assumed to be constant throughout our analysis. Although an analytical solution of the above Schrödinger equation is not available, a sufficiently accurate solution can be found in the following way. The CDW potential has off-diagonal matrix elements

$$\langle \mathbf{k} \pm \mathbf{Q} | U^{\mathrm{CDW}} | \mathbf{k} \rangle = G/2 . \tag{2.4}$$

When $k_z \cong -Q/2$, the mixing of $|\mathbf{k}\rangle$ and $|\mathbf{k}-\mathbf{Q}\rangle$ can be treated using nondegenerate perturbation theory, but the energy difference between these two states is so large that the mixing can be neglected. However, the energy difference between $|\mathbf{k}\rangle$ and $|\mathbf{k}+\mathbf{Q}\rangle$ is a very small, so the mixing between these must be treated using degenerate perturbation theory. This leads, of course, to an energy gap at $k_z = -Q/2$. In the following analysis, only those states below the gap need be considered.

The secular equation for Eq. (2.3) becomes

$$\begin{vmatrix} \varepsilon_k' - \varepsilon_k^0 & \dfrac{G}{2} \\ \dfrac{G}{2} & \varepsilon_{k+Q}' - \varepsilon_k^0 \end{vmatrix} = 0 , \tag{2.5}$$

where $\varepsilon_k' = \hbar^2 k^2/2m$, the energy of a free electron with wave vector $\mathbf{k}$. The energy for a state below the energy gap is found from the forgoing secular equation:

$$\varepsilon_k^0 = \tfrac{1}{2}(\varepsilon_k' + \varepsilon_{k+Q}') - \tfrac{1}{2}[(\varepsilon_k' - \varepsilon_{k+Q}')^2 + G^2]^{1/2} . \tag{2.6}$$

The corresponding eigenfunction is

$$\Psi_k = \cos\phi_k e^{i\mathbf{k}\cdot\mathbf{r}} - \sin\phi_k e^{i(\mathbf{k}+\mathbf{Q})\cdot\mathbf{r}} , \tag{2.7}$$

where $\cos\phi_k = G/[G^2 + 4(\varepsilon_k' - \varepsilon_k^0)^2]^{1/2}$. These solutions will reduce to those found using nondegenerate perturbation theory when k_z is far away from $-Q/2$.

A similar solution can be found for $k_z \cong Q/2$;

$$\varepsilon_k^0 = \tfrac{1}{2}(\varepsilon_k' + \varepsilon_{k-Q}') - \tfrac{1}{2}[(\varepsilon_k' - \varepsilon_{k-Q}')^2 + G^2]^{1/2} , \tag{2.8}$$

$$\Psi_k = \cos\phi_k e^{i\mathbf{k}\cdot\mathbf{r}} - \sin\phi_k e^{i(\mathbf{k}-\mathbf{Q})\cdot\mathbf{r}} . \tag{2.9}$$

If dimensionless quantities u, v, and w are defined

$$u = k_x/Q, \quad v = k_y/Q, \quad w = k_z/Q - \frac{1}{2} \frac{k_z}{|k_z|} , \tag{2.10}$$

the above two solutions for $k_z \lessgtr 0$ can be put in a very simple form:

$$\varepsilon_k^0 = \frac{\hbar^2 Q^2}{2m} [u^2 + v^2 + \tfrac{1}{4} - (w^2 + \xi^2)^{1/2}] , \tag{2.11}$$

$$\Psi_k = \cos\phi_k e^{i\mathbf{k}\cdot\mathbf{r}} - \sin\phi_k e^{i(\mathbf{k}\pm\mathbf{Q})\cdot\mathbf{r}} , \tag{2.12}$$

$$\xi = \frac{mG}{\hbar^2 Q^2} . \tag{2.13}$$

The Fermi-surface velocity in the z direction along $\mathbf{Q}$ is given by

$$v_z = \frac{1}{\hbar} \frac{\partial \varepsilon_k^0}{\partial k_z} = \frac{\hbar Q}{m} \left[w - \frac{w}{2(w^2 + \xi^2)^{1/2}} \right] . \tag{2.14}$$

When $w \cong 0$, i.e., near $k_z \cong \pm Q/2$, the electron velocity nearly vanishes. An approximate shape of the Fermi surface can be obtained by requiring critical contact between the Fermi surface and two CDW gaps (of magnitude G).[17] It follows from this assumption that

$$\varepsilon_k^0 = \varepsilon_F = \frac{\hbar^2 (Q/2)^2}{2m} - \frac{G}{2} , \tag{2.15}$$

$$\kappa \equiv (u^2 + v^2)^{1/2} = [(w^2 + \xi^2)^{1/2} - \xi - w^2]^{1/2} . \tag{2.16}$$

The Fermi surface is then distorted into the shape of a lemon, as shown in Fig. 1.

When the crystal potential is also included, the Schrödinger equation becomes

$$\left[\frac{p^2}{2m} + G \cos\mathbf{Q} \cdot \mathbf{r} + V \cos\mathbf{G} \cdot \mathbf{r} \right] \Psi_k = \varepsilon_k^0 \Psi_k . \tag{2.17}$$

Solution of the above Schrödinger equation leads to energy gaps at the Brillouin-zone faces perpendicular to $\mathbf{G}$ as well as the main CDW gaps. In addition, there are new gaps corresponding to $\mathbf{K}_{m,n} = m\mathbf{Q} + n\mathbf{G}$ with $-\infty \le m < \infty$ and $-\infty \le n < \infty$. Among these only the following three groups of lower-order gaps are important. Since
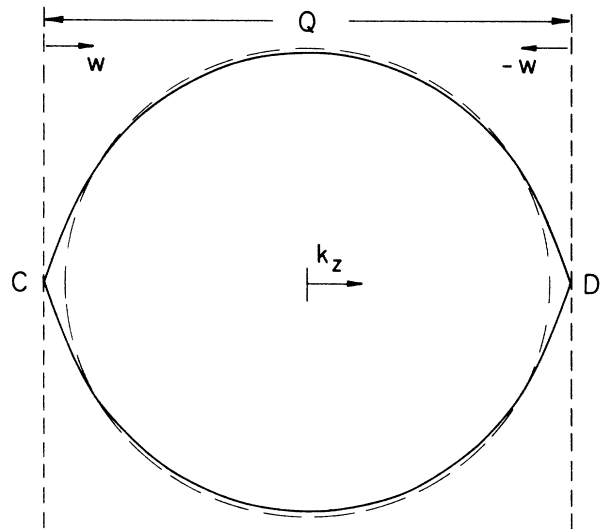

FIG. 1. Lemon-shaped Fermi surface for $G/E_F = 0.5$. The dashed curve is that of a free-electron Fermi sphere, of radius k_F, having the same volume as the lemon-shaped surface. The dashed curve is drawn $\frac{4}{3}\%$ larger than actual.
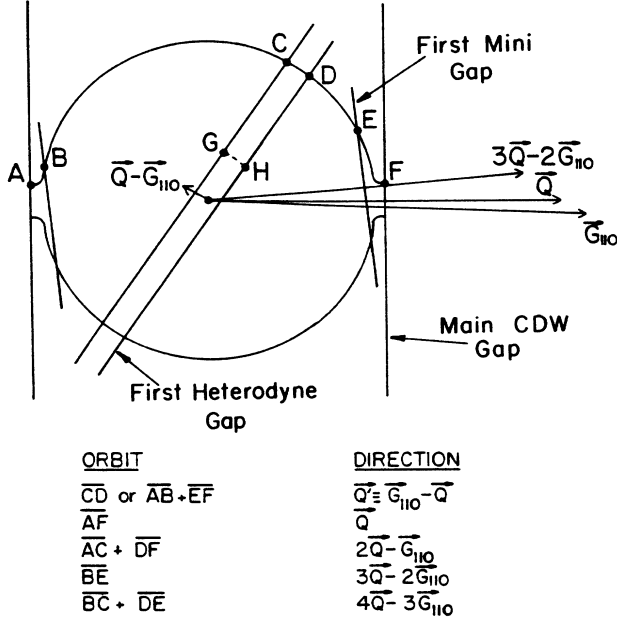
FIG. 2. Fermi surface, energy gaps, and open orbits (for **H** perpendicular to the plane shown).

$Q' \equiv G - Q$ is very small, the size of the gaps falls off rapidly with increasing n.[18] The three groups of lower-order gaps are (a) first-zone minigaps; $\mathbf{K}_{n+1,-n} = (n+1)\mathbf{Q} - n\mathbf{G}$, (b) second-zone minigaps; $\mathbf{K}_{-n,n+1} = (n+1)\mathbf{G} - n\mathbf{Q}$, and (c) heterodyne gaps; $\mathbf{K}_{-n,n} = n(\mathbf{G}-\mathbf{Q})$, where $n = 1,2,3,. . . .$. Minigaps and heterodyne gaps truncate the Fermi surface so that open orbits become possible. Five possible open orbits (depending on magnetic breakdown) are depicted in Fig. 2.

Since the optimum direction of **Q** does not coincide with a symmetry axis, there are 24 equivalent directions in a single crystal.[19] In general, a macroscopic sample will be divided into **Q** domains, and this plays a very important role in explaining spin-wave data. In the analysis that follows, only consequences of distortion of the Fermi surface, the presence of open orbits, and domain structure will be considered.

III. BRIEF REVIEW
OF LANDAU FERMI-LIQUID THEORY

Landau Fermi-liquid theory[20,21] is based on the assumption that energy levels of an interacting Fermi system can be classified in the same way as the corresponding noninteracting system. That is, a state in the noninteracting system characterized by momentum **p** is assumed to evolve in some way to a corresponding state in the interacting system as the interaction is gradually turned on, and to remain characterized by the same momentum **p**. A state in the interacting system is called a quasiparticle or an elementary excitation, and can be considered as a single particle surrounded by a self-consistent distribution of other particles. A quasiparticle has the same charge as the corresponding noninteracting

particle, and they obey Fermi statistics.

Since the energy of a particle depends on the states of the surrounding particles, the total energy of the system becomes a functional of the distribution function $f(\mathbf{p})$, which is envisioned as a statistical matrix with respect to spin. It is assumed that the distribution $f(\mathbf{p})$ characterizes the system completely. For an infinitesimal change in the distribution function $\delta f(\mathbf{p})$ the change in the total energy is expanded to second order in $\delta f(\mathbf{p})$. We shall take the volume of the system to be unity.

$$\delta E = \mathrm{Tr} \int \varepsilon_0(\mathbf{p})\delta f(\mathbf{p}) \frac{d\mathbf{p}}{(2\pi\hbar)^3}$$

$$+ \tfrac{1}{2}\mathrm{Tr}\, \mathrm{Tr}' \int F(\mathbf{p},\mathbf{p}')\delta f(\mathbf{p})\delta f(\mathbf{p}') \frac{d\mathbf{p}}{(2\pi\hbar)^3} \frac{d\mathbf{p}'}{(2\pi\hbar)^3}$$

$$= \mathrm{Tr} \int \varepsilon(\mathbf{p})\delta f(\mathbf{p}) \frac{d\mathbf{p}}{(2\pi\hbar)^3} , \qquad (3.1)$$

where

$$\varepsilon(\mathbf{p}) = \varepsilon_0(\mathbf{p}) + \mathrm{Tr}' \int F(\mathbf{p},\mathbf{p}')\delta f(\mathbf{p}') \frac{d\mathbf{p}'}{(2\pi\hbar)^3} . \qquad (3.2)$$

$\varepsilon(\mathbf{p})$ is the functional derivative of the total energy E with respect to $\delta f(\mathbf{p})$ and corresponds to a change in the energy of the system upon the addition of a single quasiparticle with momentum **p**; $\varepsilon(\mathbf{p})$ is the energy of the quasiparticle and $\varepsilon_0(\mathbf{p})$ is the energy in the equilibrium distribution. $F(\mathbf{p},\mathbf{p}')$ is the second-order functional derivative of the total energy with respect to the distribution function, and can be considered as the interaction function between quasiparticles.

Since there is a one-to-one correspondence between a state in the interacting system and the corresponding state in the noninteracting system, the entropy of the interacting system can be obtained in the same way as in the noninteracting system.

$$S = -\mathrm{Tr} \int [f \ln f + (1-f)\ln(1-f)] \frac{d\mathbf{p}}{(2\pi\hbar)^3} . \qquad (3.3)$$

Using the thermodynamic law

$$\delta E = T\delta S + \mu\delta N , \qquad (3.4)$$

one can get the distribution function for the quasiparticles, where N is the number of quasiparticles and μ is the chemical potential,

$$f(\mathbf{p}) = \frac{1}{e^{[\varepsilon(\mathbf{p})-\mu]/kT}+1} , \qquad (3.5)$$

where μ is the chemical potential and is equal to Fermi energy $\varepsilon_F = \varepsilon(p_F)$ at zero temperature. The assignment of a definite momentum to each quasiparticle is possible only when the uncertainty in the momentum due to the finite mean free path is small compared with the momentum and the width of the "transition zone" of the distribution. This leads to the following condition.[22]

$$kT \ll \varepsilon_F . \qquad (3.6)$$

Nonequilibrium states of a Fermi liquid are described by a distribution function $f(\mathbf{p},\mathbf{r},t)$ which depends on both position **r** and momentum **p**, which gives the distri-

Table

ORBIT	DIRECTION
$\overline{CD}$ or $\overline{AB} + \overline{EF}$	$\overline{Q} \equiv \overline{G}_{110} - \overline{Q}$
$\overline{AF}$	$\overline{Q}$
$\overline{AC} + \overline{DF}$	$2\overline{Q} - \overline{G}_{110}$
$\overline{BE}$	$3\overline{Q} - 2\overline{G}_{110}$
$\overline{BC} + \overline{DE}$	$4\overline{Q} - 3\overline{G}_{110}$

bution in a unit volume centered at $\mathbf{r}$. This description is valid as long as the quasiparticle de Broglie wavelength $\hbar/p_F$ is small compared to the wavelength of the inhomogeneity λ,

$$\frac{\hbar}{p_F} \ll \lambda, \quad \text{or} \quad \hbar q \ll p_F . \tag{3.7}$$

Since the frequency ω of the inhomogeneity is of order $v_F q$, the above criterion is equivalent to[22]

$$\hbar\omega \ll \varepsilon_F . \tag{3.8}$$

Therefore Landau theory is applicable only to macroscopic disturbances. Now the change in the total energy becomes

$$\delta E = \mathrm{Tr} \int \int \varepsilon_0(\mathbf{p})\delta f(\mathbf{p},\mathbf{r},t)\frac{d\mathbf{p}}{2\pi\hbar)^3}d\mathbf{r}$$
$$+ \tfrac{1}{2}\mathrm{Tr}\,\mathrm{Tr}' \int \int F(\mathbf{p},\mathbf{r},\mathbf{p}',\mathbf{r}')\delta f(\mathbf{p},\mathbf{r},t)$$
$$\times\delta f(\mathbf{p}',\mathbf{r}',t)\frac{d\mathbf{p}}{(2\pi\hbar)^3}\frac{d\mathbf{p}'}{(2\pi\hbar)^3}d\mathbf{r}d\mathbf{r}'$$
$$=\mathrm{Tr}\int\varepsilon(\mathbf{p},\mathbf{r},t)\delta f(\mathbf{p},\mathbf{r},t)\frac{d\mathbf{p}}{(2\pi\hbar)^3}d\mathbf{r} , \tag{3.9}$$

where

$$\varepsilon(\mathbf{p},\mathbf{r},t)=\varepsilon_0(\mathbf{p})+\delta\varepsilon(\mathbf{p},\mathbf{r},t) , \tag{3.10}$$

and

$$\delta\varepsilon(\mathbf{p},\mathbf{r},t)=\mathrm{Tr}'\int F(\mathbf{p},\mathbf{r},\mathbf{p}',\mathbf{r}')\delta f(\mathbf{p}',\mathbf{r},t)\frac{d\mathbf{p}'}{(2\pi\hbar)^3}d\mathbf{r}' . \tag{3.11}$$

When the system is assumed to be invariant under spatial translation, the interaction function can only depend on $(\mathbf{r}-\mathbf{r}')$:

$$F(\mathbf{p},\mathbf{r},\mathbf{p}',\mathbf{r}')=F(\mathbf{p},\mathbf{p}',\mathbf{r}-\mathbf{r}') . \tag{3.12}$$

When the interaction is of short range,

$$\delta\varepsilon(\mathbf{p},\mathbf{r},t)\simeq\mathrm{Tr}\int F(\mathbf{p},\mathbf{p}')\delta f(\mathbf{p}',\mathbf{r},t)\frac{d\mathbf{p}'}{(2\pi\hbar)^3} , \tag{3.13}$$

where

$$F(\mathbf{p},\mathbf{p}')=\int F(\mathbf{p},\mathbf{r},\mathbf{p}',\mathbf{r}')d\mathbf{r}' . \tag{3.14}$$

This procedure is not directly applicable to an electron system in a metal, since the Coulomb interaction is a long-range interaction. As shown by Silin,[23] this difficulty can be removed if one includes dynamic screening of the particle motion self-consistently. The electrostatic interaction between the average charge distribution of an excited quasiparticle can be described by a space-charge electrostatic field $\mathbf{E}_p(\mathbf{r},t)$ given by

$$\nabla\cdot\mathbf{E}_p(\mathbf{r},t)=4\pi e\,\mathrm{Tr}\int\delta f(\mathbf{p},\mathbf{r},t)\frac{d\mathbf{p}}{(2\pi\hbar)^3} . \tag{3.15}$$

This field can be regarded as an additional applied field. As a result, each excited quasiparticle is surrounded by a polarization cloud of other quasiparticles. The residual interaction $F(\mathbf{p},\mathbf{r},\mathbf{p}',\mathbf{r}')$ is short ranged and can be described by the above procedure. The local quasiparticle energy becomes

$$\varepsilon(\mathbf{p},\mathbf{r},t)=\varepsilon_0(\mathbf{p})+\mathrm{Tr}'\int F(\mathbf{p},\mathbf{p}')\delta f(\mathbf{p}',\mathbf{r},t)\frac{d\mathbf{p}'}{(2\pi\hbar)^3} . \tag{3.16}$$

In Landau theory, $\varepsilon(\mathbf{p},\mathbf{r},t)$ is considered as the Hamiltonian function of the quasiparticle.

The distribution function satisfies a transport equation

$$\frac{df}{dt}=I[f] , \tag{3.17}$$

where $I[f]$ is the collision integral, giving the rate of change in the distribution due to collisions. The explicit time dependence of f contributes a term $\partial f/\partial t$. The dependence on the coordinates and momenta gives terms

$$\frac{\partial f}{\partial\mathbf{r}}\cdot\frac{d\mathbf{r}}{dt}+\frac{\partial f}{\partial\mathbf{p}}\cdot\frac{d\mathbf{p}}{dt}=\frac{\partial f}{\partial\mathbf{r}}\cdot\frac{\partial\varepsilon}{\partial\mathbf{p}}-\frac{\partial f}{\partial\mathbf{p}}\cdot\frac{\partial\varepsilon}{\partial\mathbf{r}}=\{f,\varepsilon\}^{\mathrm{PB}}_{\mathbf{r},\mathbf{p}} ,$$

where Hamilton's equations have been used and PB stands for Poisson bracket. Finally, the time variation of the function as an operator with respect to the spin variables is given by $(\iota/\hbar)[\varepsilon,f]=(\iota/\hbar)[\varepsilon f-f\varepsilon]$. Collecting all the terms, one gets the Landau-Silin equation,

$$\frac{\partial f}{\partial t}+\{f,\varepsilon\}^{\mathrm{PB}}_{\mathbf{r},\mathbf{p}}+\frac{\iota}{\hbar}[\varepsilon,f]=I[f] . \tag{3.18}$$

The distribution function and quasiparticle energy can be decomposed into spin-dependent and spin-independent parts using the Pauli matrices τ:

$$f=n_1+\tau\cdot\mathbf{n}_2 , \tag{3.19}$$

$$\varepsilon=\varepsilon_1+\tau\cdot\varepsilon_2 . \tag{3.20}$$

By inserting Eqs. (3.19) and (3.20) into Eq. (3.18) and taking a trace, one gets

$$\frac{\partial n_1}{\partial t}+\{n_1,\varepsilon_1\}^{\mathrm{PB}}_{\mathbf{r},\mathbf{p}}+\{n_2^j,\varepsilon_2^j\}^{\mathrm{PB}}_{\mathbf{r},\mathbf{p}}=I[n_1] . \tag{3.21}$$

By inserting Eqs. (3.19) and (3.20) into Eq. (3.18), multiplying by τ, and taking a trace, one gets

$$\frac{\partial\mathbf{n}_2}{\partial t}\{n_1,\varepsilon_2\}^{\mathrm{PB}}_{\mathbf{r},\mathbf{p}}+\{\mathbf{n}_2,\varepsilon_1\}^{\mathrm{PB}}_{\mathbf{r},\mathbf{p}}-\frac{2}{\hbar}\varepsilon_2\times\mathbf{n}_2=I[\mathbf{n}_2] . \tag{3.22}$$

In the presence of external fields, the conjugate momentum $\mathbf{p}$ is different from the usual momentum $\mathbf{k}$:

$$\mathbf{p}=\mathbf{k}+\frac{e}{c}\mathbf{A} , \tag{3.23}$$

where one can take the gauge, $\phi=0$, without loss of generality; i.e.,

$$\mathbf{B}=\nabla\times\mathbf{A}, \quad \mathbf{E}=-\frac{1}{c}\frac{\partial\mathbf{A}}{\partial t} . \tag{3.24}$$

It is more convenient to express the transport equations in terms of $\mathbf{k}$, which has physical meaning in the absence of external fields.[21] The effect of the vector potential $\mathbf{A}$ is to shift the origin in $\mathbf{p}$ space by an amount $e\mathbf{A}/c$. $\mathbf{p}$ is

measured from this shifted origin, and the distribution function $f(\mathbf{p},\mathbf{r},t)$ is the same as the distribution $f(\mathbf{k},\mathbf{r},t)$ measured from the true origin $\mathbf{k}=0$. If the Hamiltonian is expressed in terms of $\mathbf{k}$ and $\mathbf{r}$, it has the same form as when $\mathbf{A}=0$ and $\mathbf{p}=\mathbf{k}$. Now express everything in terms of $\mathbf{k}$ and $\mathbf{r}$;

$$\mathbf{k}=\mathbf{p}-\frac{e}{c}\mathbf{A} \ . \tag{3.25}$$

For operators M and N which depend on $\mathbf{p}$ and $\mathbf{r}$,

$$\left[\frac{\partial M}{\partial t}\right]_{\mathbf{p},\mathbf{r}}=\frac{\partial M}{\partial t}+e\mathbf{E}\cdot\frac{\partial M}{\partial \mathbf{k}} \ , \tag{3.26}$$

$$\{M,N\}^{\mathrm{PB}}_{\mathbf{r},\mathbf{p}}=\{M,N\}^{\mathrm{PB}}_{\mathbf{r},\mathbf{k}}+\frac{e}{c}\frac{\partial M}{\partial \mathbf{k}}\times\frac{\partial N}{\partial \mathbf{k}}\cdot\mathbf{B} \ . \tag{3.27}$$

The transport equations become

$$\frac{\partial n_1}{\partial t}+\{n_1,\varepsilon_1\}^{\mathrm{PB}}_{\mathbf{r},\mathbf{k}}+\{n_2^j,\varepsilon_2^j\}^{\mathrm{PB}}_{\mathbf{r},\mathbf{k}}$$
$$+e\left[\mathbf{E}+\frac{1}{c}\frac{\partial \varepsilon_1}{\partial \mathbf{k}}\times\mathbf{B}\right]\cdot\frac{\partial n_1}{\partial \mathbf{k}}+\frac{e}{c}\frac{\partial n_2^j}{\partial \mathbf{k}}\times\frac{\partial \varepsilon_2^j}{\partial \mathbf{k}}\cdot\mathbf{B}=I[n_1] \ , \tag{3.28}$$

where the summation over repeated indices is assumed;

$$\frac{\partial \mathbf{n}_2}{\partial t}+\{\mathbf{n}_2,\varepsilon_1\}^{\mathrm{PB}}_{\mathbf{r},\mathbf{k}}+\{n_1,\varepsilon_2\}^{\mathrm{PB}}_{\mathbf{r},\mathbf{k}}-\frac{2}{\hbar}\varepsilon_2\times\mathbf{n}_2$$
$$+e\left[\mathbf{E}+\frac{1}{c}\frac{\partial \varepsilon_1}{\partial \mathbf{k}}\times\mathbf{B}\right]\cdot\nabla_\mathbf{k}\mathbf{n}_2-\frac{e}{c}\frac{\partial n_1}{\partial \mathbf{k}}\times\mathbf{B}\cdot\frac{\partial \varepsilon_2}{\partial \mathbf{k}}=I[\mathbf{n}_2] \ . \tag{3.29}$$

When the system is invariant under translation and there is no spin-orbit coupling, the interaction function $F(\mathbf{k},\mathbf{k}')$ can be decomposed into spin-independent and spin-dependent parts in terms of Pauli spin matrices,[5,21]

$$F(\mathbf{k},\mathbf{k}')=\eta(\mathbf{k},\mathbf{k}')+\boldsymbol{\tau}\cdot\boldsymbol{\tau}'\zeta(\mathbf{k},\mathbf{k}') \ . \tag{3.30}$$

Under the presence of a static field $\mathbf{H}_0$ and an rf field $\mathbf{h}$,

$$\varepsilon_1=\varepsilon_\mathbf{k}^0+\int\frac{2d\mathbf{k}'}{(2\pi\hbar)^3}\eta(\mathbf{k},\mathbf{k}')n_1(\mathbf{k}',\mathbf{r},t) \ , \tag{3.31}$$

$$\varepsilon_2=-\frac{\gamma_0\hbar}{2}\mathbf{H}+\int\frac{2d\mathbf{k}'}{(2\pi\hbar)^3}\zeta(\mathbf{k},\mathbf{k}')\mathbf{n}_2(\mathbf{k}',\mathbf{r},t) \tag{3.32}$$

$$=\varepsilon_2^0+\delta\varepsilon_2 \ , \tag{3.33}$$

where

$$\varepsilon_2^0=-\frac{\gamma\hbar}{2}\mathbf{H}_0 \ , \tag{3.34}$$

$$\gamma=\gamma_0/\gamma_0^B \ , \tag{3.35}$$

$$\gamma_0^B=1+B_0 \ , \tag{3.36}$$

$$B_0=\int\frac{2d\mathbf{k}'}{(2\pi\hbar)^3}\zeta(\mathbf{k},\mathbf{k}')\frac{\partial n_{\mathbf{k}'}^0}{\partial \varepsilon_{\mathbf{k}'}^0} \ , \tag{3.37}$$

and γ_0 is the gyromagnetic ratio of an electron. In terms of these quantities, one can linearize the transport equation for spin polarizations m_α $(\alpha=+,-,0)$, where $m_\pm=(m_x\pm im_y)/\sqrt{2}$ and $m_0=m_z$. The linearized Landau-Silin equation is

$$\frac{\partial m_\alpha}{\partial t}+\frac{e}{c}\mathbf{v}_\mathbf{k}\times\mathbf{H}_0\cdot\left[\frac{\partial m_\alpha}{\partial \mathbf{k}}-\frac{\partial n_\mathbf{k}^0}{\partial \varepsilon_\mathbf{k}^0}\frac{\partial\delta\varepsilon_{2\alpha}}{\partial \mathbf{k}}\right]+\mathbf{v}_\mathbf{k}\cdot\nabla\left[m_\alpha-\frac{\partial n_\mathbf{k}^0}{\partial \varepsilon_\mathbf{k}^0}\delta\varepsilon_{2\alpha}\right]-i\alpha\Omega_0\left[m_\alpha-\frac{\partial n_\mathbf{k}^0}{\partial \varepsilon_\mathbf{k}^0}\delta\varepsilon_{2\alpha}\right]=I[m_\alpha] \ , \tag{3.38}$$

where

$$\Omega_0=-\gamma H_0 \ , \tag{3.39}$$

and

$$\delta\varepsilon_{2\alpha}=-\frac{\gamma_0\hbar}{2}h_\alpha+\int\frac{2d\mathbf{k}'}{(2\pi\hbar)^3}\zeta(\mathbf{k},\mathbf{k}')m_\alpha(\mathbf{k}',\mathbf{r},t) \ . \tag{3.40}$$

IV. SIMPLIFIED MODEL FOR CHARGE-DENSITY-WAVE EFFECTS

In the following analysis, several CDW effects[8] will be incorporated into the theory of spin waves in alkali metals; mainly, the anisotropic velocity distribution caused by the distortion of the Fermi surface, the open-orbit motion resulting from truncation of the Fermi surface by the extra energy gaps, and CDW Q-domain structure. Among many possible open orbits, the ones due to the heterodyne gaps are believed to be most important, since its direction has the largest angle with respect to $\mathbf{Q}$. Also

it is believed that $\mathbf{G}_{110}$ is usually perpendicular to the surface of a thin sample.[24]

The above three effects will be analyzed using the following simplified model, shown in Fig. 3. The Fermi surface can be thought of as being composed of two parts: a lemon-shaped surface and a cylindrical surface. The lemon-shaped surface describes the motion of electrons in closed orbits and the cylindrical surface describes the motion of electrons in open orbits. The axis of the cylin-
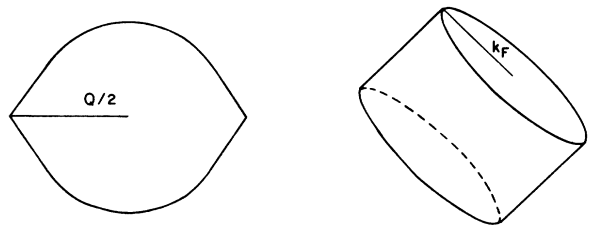

FIG. 3. Simplified model of the Fermi surface.

drical surface is taken parallel to $Q' = G_{110} - Q$.

In the following analysis, B_n with $n \geq 1$ will be neglected since they are believed to be quite small compared to B_0.[11] Instead, we will introduce η, the fraction of electrons in the cylindrical part, as a new parameter. It should be emphasized that G, the CDW energy gap, and Q, the CDW wave vector, are not parameters to be used in fitting the spin-wave data. They are determined from other experiments.[8] So we have B_0 and η as fitting parameters instead of B_0 and B_1 as in conventional theories. If η were to become known from another experiment, we could include B_1 as an adjustable parameter. We emphasize that B_1 and η play compensatory roles. Determinations of B_1 from spin-wave data have significance only if a CDW structure is not present.

A. Closed orbits

For the closed-orbit part, the energy of an electron is given by

$$\varepsilon_k^{0,c} = \frac{1}{2m}(k_x^2 + k_y^2) + \frac{\hbar^2 Q^2}{2m} f_e(w) , \tag{4.1}$$

where (x,y,z) refers to the c-coordinate system defined in Fig. 4 with $\hat{z}$ parallel to $\hat{Q}$, the superscript c stands for closed orbit, m is the band mass $(m = 1.211 m_0)$, and

$$f_e(w) = w^2 + \frac{1}{4} - (w^2 + \xi^2)^{1/2} , \tag{4.2}$$

$$w = \frac{k_z}{\hbar Q} \mp \frac{1}{2}\text{sgn}(k_z) , \tag{4.3}$$

$$\xi = \frac{mG}{\hbar^2 Q^2} = 0.003525 . \tag{4.4}$$

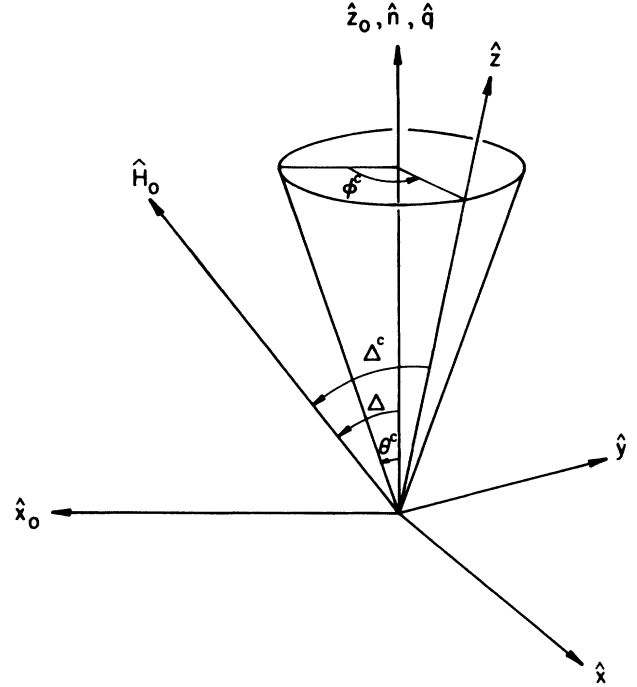(This value of ξ falls a little short of critical contact of the

FIG. 4. Definitions of coordinate systems and angles.

Fermi surface with the CDW gap.) The coordinate systems used and angles are defined in Fig. 4, where Q is parallel to $\hat{z}$. Since m_α^c in Eq. (3.38) is proportional to $\partial n_k^{c,0} / \partial \varepsilon_k^{c,0}$, it is convenient to define

$$m_\alpha^c = -\frac{\partial n_k^{c,0}}{\partial \varepsilon_k^{c,0}} g_\alpha^c . \tag{4.5}$$

The Landau-Silin equation becomes

$$\delta(\varepsilon_k^{0,c} - \varepsilon_F)\left[\omega g_\alpha^c - \Omega_0 \bar{g}_\alpha^c + \frac{\iota}{\tau}(\bar{g}_\alpha^c - \langle \bar{g}_\alpha^c \rangle^c) + \frac{\iota}{T_2}\bar{g}_\alpha^c + \iota \mathbf{v} \cdot \nabla \bar{g}_\alpha^c\right] + \iota \frac{e}{c}\left[\mathbf{v} \times \mathbf{H}_0 \cdot \frac{\partial}{\partial \mathbf{k}}\right]\delta(\varepsilon_k^{0,c} - \varepsilon_F)\bar{g}_\alpha^c = 0 , \tag{4.6}$$

where $\langle \ \rangle$ denotes the average over the Fermi surface,

$$\bar{g}_\alpha^c = g_\alpha^c - \frac{\gamma_0 \hbar}{2} h_\alpha + \delta g_\alpha^c , \tag{4.7}$$

and

$$\delta g_\alpha^c = \int \frac{2 d\mathbf{k}'}{(2\pi\hbar)^3} \zeta(\mathbf{k},\mathbf{k}')\delta(\varepsilon_{k'}^{0,c} - \varepsilon_F)g_\alpha^c(\mathbf{k}') . \tag{4.8}$$

We will look for a solution of the form

$$g_\alpha^c = g_{0\alpha}^c + \mathbf{g}_{1\alpha}^c \cdot \mathbf{v} , \tag{4.9}$$

which is the simplest function with a term linear in the velocity. The rf magnetization $\mathcal{M}_\alpha^c$ is obtained by integrating m_α^c over $\mathbf{k}$:

$$\mathcal{M}_\alpha^c = \int \frac{2 d\mathbf{k}}{(2\pi\hbar)^3} \frac{\gamma_0 \hbar}{2} m_\alpha^c = \frac{\gamma_0 \hbar}{2} v_F^c g_{0\alpha}^c , \tag{4.10}$$

where v_F^c is the density of states at the Fermi energy.

It will be assumed that all fields and spin polarization depend on the coordinate $z_0 = -x \sin\theta^c + z \cos\theta^c$, where $\hat{z}_0$ is perpendicular to the surface of the sample. By integrating Eq. (4.6) over $\mathbf{k}$, after multiplying by 1, v_x, v_y, and v_z, we obtain four coupled equations for $g_{0\alpha}^c$, $g_{1\alpha x}^c$, $g_{1\alpha y}^c$, and $g_{1\alpha z}^c$:

$$\omega g_{0\alpha}^c + \left[\alpha\omega_s + \frac{\iota}{T}\right]g_{0\alpha'}^c - \iota\langle v_x^2\rangle^c \frac{\partial}{\partial x}g_{1\alpha x}^c$$

$$+ \iota\langle v_z^2\rangle^c \frac{\partial}{\partial y}g_{1\alpha z}^c = 0 , \tag{4.11}$$

$$(\bar{\omega}^c + \alpha\Omega_0)\langle v_x^2\rangle^c g_{1\alpha x}^c - \iota\omega_c \Lambda_z^c \langle v_y^2\rangle^c g_{1\alpha y}^c$$

$$+ \iota\omega_c \Lambda_z^c \langle v_z^2\rangle^c g_{1\alpha z}^c = \iota\gamma_0^B \langle v_x^2\rangle^c \frac{\partial}{\partial x}g_{0\alpha'}^c , \tag{4.12}$$

$$\iota\omega_c\Lambda_z^c\langle v_x^2\rangle^c g_{1ax}^c +(\bar\omega^c+\alpha\Omega_0)\langle v_y^2\rangle^c g_{1ay}^c$$

$$-\iota\omega_c\Lambda_x^c\langle v_z^2\rangle^c g_{1az}^c=0 , \quad (4.13)$$

$$-\iota\omega_c\Lambda_y^c\Big\langle v_x^2\frac{m\partial v_z}{\partial k_z}\Big\rangle^c g_{1ax}^c +\iota\omega_c\Lambda_x^c\Big\langle v_y^2\frac{m\partial v_z}{\partial k_z}\Big\rangle^c g_{1ay}^c$$

$$+(\bar\omega^c+\alpha\Omega_0)\langle v_z^2\rangle^c g_{1az}^c=\iota\gamma_0^B\langle v_z^2\rangle^c\frac{\partial}{\partial z}g_{0a}^{c'} , \quad (4.14)$$

where

$$g_{0\alpha}^{c'}=g_{0\alpha}^c-\frac{\gamma_0\hbar}{2\gamma_0^B}h_\alpha , \quad (4.15)$$

$$T=T_2/\gamma_0^B , \quad (4.16)$$

and

$$\bar\omega^c=\omega+i/\tau . \quad (4.17)$$

The Λ^c's specify the direction of H_0 in the c-coordinate system:

$$\Lambda_x^c=\sin\Delta \cos\theta^c\cos\phi^c-\cos\Delta \cos\theta^c ,$$

$$\Lambda_y^c=-\sin\Delta \sin\phi^c , \quad (4.18)$$

$$\Lambda_z^c=\sin\Delta \sin\theta^c\cos\phi^c+\cos\Delta \cos\theta^c ,$$

where Δ is the angle between H_0 and $\hat{z}_0$ (perpendicular to the surface of the sample), and θ^c and ϕ^c are the polar and azimuthal angle of Q relative to the coordinate system (x_0,x_0,z_0).

Various averages in the above equations can be evaluated to first order in ξ;

$$\langle v_x^2\rangle^c=\langle v_y^2\rangle^c=\tfrac{1}{3}v_F^2(1-2\xi) ,$$

$$\langle v_z^2\rangle^c=\tfrac{1}{3}v_F^2\left[1-2\xi\left[3\tan^{-1}\frac{1}{2\xi}-2\right]\right] , \quad (4.19)$$

$$\Big\langle v_x^2\frac{m\partial v_z}{\partial k_z}\Big\rangle^c=\Big\langle v_y^2\frac{m\partial v_z}{\partial k_z}\Big\rangle^2=\tfrac{1}{3}v_F^2[1-(3\pi+\tfrac{1}{2})\xi] .$$

A solution can be found for $g_{0\alpha}^c$ by solving Eqs. (4.11)–(4.14):

$$\omega g_{0\alpha}^c+(\alpha\omega_s+\iota/T-\gamma_0^B\beta^c\nabla_0^2)g_{0\alpha}^{c'}=0 , \quad (4.20)$$

where

$$\beta^c=\langle v_x^2\rangle^c\{\sin^2\theta^c[(\bar\omega^c+\alpha\Omega_0)^2-\mu\omega_c^2(\Lambda_x^c)^2]+\lambda \cos^2\theta^c[(\bar\omega^c+\alpha\Omega_0)^2-\omega_c^2(\Lambda_z^c)^2]$$

$$+\sin\theta^c\cos\theta^c[(\lambda+\mu)\omega_c^2\Lambda_x^c\Lambda_z^c-\iota(\lambda-\mu)\omega_c\Lambda_y^c(\bar\omega^c+\alpha\Omega_0)]\}/\{(\bar\omega^c+\alpha\Omega_0)[(\mu \sin^2\Delta^c+\cos^2\Delta^c)\omega_c^2-(\bar\omega^c+\alpha\Omega_0)^2]\},$$

$$\mu=\Big\langle v_x^2\frac{m\partial v_z}{\partial k_z}\Big\rangle^c\Big/\langle v_x^2\rangle^c , \quad (4.21)$$

By using Eqs. (4.10) and (4.20), one obtains a modified Bloch equation,

$$\omega\mathcal{M}_a^c+(\alpha\omega_s+\iota/T-\gamma_0^B\beta^c\nabla_0^2)(\mathcal{M}_\alpha^c-\chi h_\alpha)=0 , \quad (4.22a)$$

or equivalently

$$\frac{\partial M}{\partial t}=\gamma_0 M\times H-\frac{M-M_{eq}}{T}+D^c\nabla_0^2(M-M_{eq}) , \quad (4.22b)$$

where $M_{eq}=\chi H=\chi(H_0+h)$, $M=M_{eq}+\mathcal{M}^c$, $D^c=\gamma_0^B\beta^c/\iota$, and $\chi=\chi_0/\gamma_0^B$ is the susceptibility of an interacting electron gas. Equation (4.22), originally suggested by Torrey,[25] was first obtained by Walker.[7] When fields and spin polarizations are assumed to be proportional to $e^{\iota q z_0}$, Eq. (4.20) is reduced to

$$g_{0\alpha}^c=\frac{\Omega_0\dfrac{\gamma_0\hbar}{2}\left[\alpha+\dfrac{\iota}{\Omega_0 T}+\dfrac{\beta^c q^2}{\Omega_0}\right]h_\alpha}{\omega+\alpha\omega_s+\iota/T+\gamma_0^B\beta^c q^2} . \quad (4.23)$$

By neglecting terms of the order $1/\Omega_0 T\ll1$ and $\beta^c q^2/\Omega_0\ll1$, in the small-q limit, one gets

$$g_{0\alpha}^c=\frac{\alpha\Omega_0\dfrac{\gamma_0\hbar}{2}h_\alpha}{\omega+\alpha\omega_s+\iota/T+\gamma_0^B\beta^c q^2} , \quad (4.24)$$

which was first obtained by Platzman and Wolff.[5] The Bloch equation in this limit is

$$\omega\mathcal{M}_\alpha^c+(\alpha\omega_s+\iota/T-\gamma_0^B\beta^c\nabla_0^2)\mathcal{M}_\alpha^c=\alpha\omega_s\chi h_\alpha , \quad (4.25a)$$

or equivalently

$$\frac{\partial M}{\partial t}=\gamma_0 M\times H-\frac{M-M_0}{T}+D^c\nabla_0^2 M , \quad (4.25b)$$

where $M_0=\chi H_0$ and $M=M_0+\mathcal{M}^c$. Equation (4.22) is more accurate than Eq. (4.25) in the sense that no specific spatial dependence of fields and polarizations is assumed. It has the nice property that the magnetization relaxes to the local equilibrium value χH, and it is valid for all α. But Eq. (4.25), originally suggested by Kaplan,[26] would be equally satisfactory for our purpose, since only small-q excitations are of interest and only the $\alpha=-1$ component is resonant. Equation (4.22a) can be put in a slightly different form in terms of $\mathcal{M}_\alpha^{c'}$:

$$\omega \mathcal{M}_\alpha^{c'} + (\alpha\omega_s + \iota/T - \gamma_0^B \beta^c \nabla_0^2)\mathcal{M}_\alpha^{c'} = -\left[\frac{\omega}{\omega_s}\right]\omega_s \chi h_\alpha \ ,$$

(4.26)

where

$$\mathcal{M}_\alpha^{c'} = \mathcal{M}_\alpha^c - \chi h_\alpha \ .$$

(4.27)

Since $\omega \cong \omega_s$, one can see that the Platzman-Wolff solution for M_- is valid without the small-q approximation if the rf magnetization in Eq. (4.25) is interpreted as the deviation from a local equilibrium value χh_- and h_- is replaced by $(\omega/\omega_s)h_- (\cong h_-)$.

When $\xi = 0$, i.e., for a spherical Fermi surface, Eq. (4.21) reduces to that of the PW theory:

$$\beta^{PW} = \beta^c \gamma_0^B = \tfrac{1}{3}v_F^2 \gamma_0^\beta(\overline{\omega}^c - \Omega_0)$$

$$\times \left[\frac{\sin^2\Delta}{\omega_c^2 - (\overline{\omega}^c - \Omega_0)^2} - \frac{\cos^2\Delta}{(\overline{\omega}^c - \Omega_0)^2}\right] \ .$$

(4.28)

If $|B_0\omega\tau/(1+B_0)| \gg 1$, β approaches a pure (real) number and g_0 exhibits a branch of singularities along the curve $\omega - \omega_s + \beta q^2 = 0$ in $\omega - q$ space. When $B_0 \to 0$, β approaches a pure imaginary number and there are no singularities. Therefore paramagnetic spin waves exist only when the interaction between electrons is strong enough.[5]

B. Open orbits

Similar procedures to those just described can be followed for the cylindrical Fermi-energy surface defined by

$$\varepsilon_\mathbf{k}^{0,o} = \frac{1}{2m}(k_x^2 + k_y^2) \ ,$$

(4.29)

where the superscript o stands for open orbit. The coordinate systems and angles used are defined in Fig. 4, where $\mathbf{Q}'$ is parallel to $\hat{\mathbf{z}}$.

The Landau-Silin equation becomes

$$\delta(\varepsilon_\mathbf{k}^{0,o} - \varepsilon_F)\left[\omega g_0^o - \Omega_0\overline{g}_\alpha^o + \frac{\iota}{\tau_{op}}(\overline{g}_\alpha^o - \langle\overline{g}_\alpha^o\rangle) + \frac{\iota}{T_2}\overline{g}_\alpha^o - \iota\mathbf{v}\cdot\nabla\overline{g}_\alpha^o\right] + \iota\frac{e}{c}\left[\mathbf{v}\times\mathbf{H}_0\cdot\frac{\partial}{\partial\mathbf{k}}\right]\delta(\varepsilon_\mathbf{k}^{0,o} - \varepsilon_F)\overline{g}_\alpha^o = 0 \ ,$$

(4.30)

where electrons in open orbits are assumed to have a different momentum relaxation time from that of electrons in closed orbits. We look for a solution having the form

$$g_\alpha^o = g_{0\alpha}^o + \mathbf{g}_{1\alpha}^o\cdot\mathbf{v} \ ,$$

(4.31)

as before. The rf magnetization $\mathcal{M}_\alpha^o$ is obtained by integrating m_α^o over $\mathbf{k}$;

$$\mathcal{M}_\alpha^o = \frac{\gamma_0\hbar}{2}v_F^o g_{0\alpha}^o \ .$$

(4.32)

It will be assumed that all fields and the spin polarization depend on the coordinate $z_0 = -x\sin\theta^o + z\cos\theta^o$. (x,y,z) refers to the c-coordinate system defined in Fig. 4 with $\hat{\mathbf{z}}$ parallel to $\hat{\mathbf{Q}}'$.

By integrating Eq. (4.30), after multiplying by $1, v_x, v_y$, we obtain three coupled equations in $g_{0\alpha}^o, g_{1\alpha x}^o, g_{1\alpha y}^o$;

$$\omega g_{0\alpha}^o + (\alpha\omega_s + \iota/T)g_{0\alpha}^{o'} - \iota\langle v_x^2\rangle^o\frac{\partial}{\partial x}g_{1\alpha x}^o = 0 \ ,$$

(4.33)

$$(\overline{\omega}^o + \alpha\Omega_0)\langle v_x^2\rangle^o g_{1\alpha x}^o - \iota\omega_c\Lambda_z^o\langle v_y^2\rangle^o g_{1\alpha y}^o$$

$$= \tfrac{1}{2}\iota\gamma_0^B\langle v_x^2\rangle^o\frac{\partial}{\partial x}g_{0\alpha}^{o'} \ ,$$

(4.34)

$$\iota\omega_c\Lambda_z^o\langle v_x^2\rangle^o g_{1\alpha x}^o + (\overline{\omega}^o + \alpha\Omega_0)\langle v_y^2\rangle^o g_{1\alpha y}^o = 0 \ ,$$

(4.35)

where $\overline{\omega}^o = \omega + \iota/\tau_{op}$. The Λ^os, defined by equations similar to (4.18), specify the direction of $\mathbf{H}_0$ in the o-coordinate system and θ^o and ϕ^o are the polar and azimuthal angle of $\hat{\mathbf{Q}}'$ relative to the coordinate system (x_0, y_0, z_0). A solution can be found for $g_{0\alpha}^o$ by using Eqs. (4.33)–(4.35):

$$\omega g_{0\alpha}^o + (\alpha\omega_s + \iota/T - \gamma_0^B\beta^o\nabla_0^2)g_{0\alpha}^{o'} = 0 \ ,$$

(4.36)

$$\beta^o = \tfrac{1}{2}v_F^2(\overline{\omega}^o - \Omega_0)\frac{\sin^2\theta^o}{\omega_p^2 - (\overline{\omega}^o - \Omega_0)^2} \ ,$$

(4.37)

where

$$\omega_p = \omega_c\cos(\hat{\mathbf{Q}}'\cdot\hat{\mathbf{H}}_0)$$

(4.38)

and

$$\overline{\omega}^o = \omega + i/\tau_{op} \ .$$

(4.39)

By using Eqs. (4.32) and (4.36), one gets Bloch equations corresponding to Eqs. (4.22) and (4.25).

The main difference between the solution here and the one in Sec. IV A is the following: The factor 3 or 2 corresponds to the dimensional freedom of the motion; an average of one component of $\mathbf{v}$ is reduced from $\tfrac{1}{3}v_F^2$ to $\tfrac{1}{2}v_F^2\sin^2\theta^o$. The electrons on the cylindrical part of the Fermi surface cannot move perpendicular to $\mathbf{Q}'$, and can only move in open orbits if $\mathbf{H}_0$ is perpendicular to $\mathbf{Q}'$. ω_c^o, the effective cyclotron frequency, becomes 0 in that case.

C. Mixed orbits

When we consider both Fermi surfaces at the same time, the cross relaxation of quasiparticles from one surface to another becomes important. When a quasiparticle is destroyed at a point on the Fermi surface, it can end up at a point on either surface with equal probability per unit Fermi-surface area. The collision integral becomes the following:

$$\left[\frac{\partial g_\alpha^c}{\partial t}\right]_{coll} = -\frac{\bar{g}_\alpha^c}{\tau} - \frac{\bar{g}_\alpha^c}{T_2} + (1-\eta)\frac{\langle \bar{g}_\alpha^c\rangle^c}{\tau} + \eta\frac{\langle \bar{g}_\alpha^o\rangle^o}{\tau_{op}} ,$$

(4.40)

$$\left[\frac{\partial g_\alpha^o}{\partial t}\right]_{coll} = -\frac{\bar{g}_\alpha^o}{\tau_{op}} - \frac{\bar{g}_\alpha^o}{T_2} + (1-\eta)\frac{\langle \bar{g}_\alpha^c\rangle^c}{\tau} + \eta\frac{\langle \bar{g}_\alpha^o\rangle^o}{\tau_{op}} ,$$

(4.41)

where η is the fraction of electrons on the open-orbit Fermi surface and τ_{op} is their momentum relaxation time. It has been shown that τ_{op} is shorter than τ on account of Q-domain boundaries:[27]

$$\frac{1}{\tau_{op}} = \frac{1}{\tau} + \frac{8v_F}{3D} ,$$

(4.42)

where D is the Q-domain size. η and D play crucial roles

in explaining the splittings of spin-wave side bands as will be shown later. In addition to the coupling through Eqs. (4.40) and (4.41), g^c and g^o get coupled through the interaction between electrons:

$$\delta g_\alpha^c = \delta g_\alpha^o = B_0[(1-\eta)g_{0\alpha}^c + \eta g_{0\alpha}^o] .$$

(4.43)

The rf magnetization $\mathcal{M}_\alpha$ is obtained by integrating m_α over $\mathbf{k}$:

$$\mathcal{M}_\alpha = \frac{\gamma_0\hbar}{2}v_F([(1-\eta)g_{0\alpha}^c + \eta g_{0\alpha}^o] .$$

(4.44)

Now we will have seven coupled equations, similar to Eqs. (4.11)–(4.13) and (4.33)–(4.35) with modified collision terms (4.40) and (4.41), and modified interaction terms Eq. (4.43), after multiplying by appropriate factors and taking averages over the Fermi surface. Solving these seven equations for g_0^c and g_0^o, one gets the following two coupled equations:

$$\omega g_{0\alpha}^c + \left[[1+(1-\eta)B_0]\left[\alpha\Omega_0+\frac{\iota}{T_2}\right] + \iota\eta\left[\frac{1+(1-\eta)B_0}{\tau} - \frac{(1-\eta)B_0}{\tau_{op}}\right]\right]g_{0\alpha}^{c'}$$

$$-\beta^c\nabla_0^2\{[1+(1-\eta)B_0]g_{0\alpha}^{c'} + \eta B_0 g_{0\alpha}^{o'}\} + \left[\eta B_0\left[\alpha\Omega_0+\frac{\iota}{T_2}\right] - \iota\eta\left[\frac{\eta B_0}{\tau} - \frac{1+\eta B_0}{\tau_{op}}\right]\right]g_{0\alpha}^{o'} = 0 ,$$

(4.45)

$$\omega g_{0\alpha}^o + \left[(1+\eta B_0)\left[\alpha\Omega_0+\frac{\iota}{T_2}\right] - \iota(1-\eta)\left[\frac{\eta B_0}{\tau} - \frac{1+\eta B_0}{\tau_{op}}\right]\right]g_{0\alpha}^{o'} - \beta^o\nabla_0^2[(1+\eta B_0)g_{0\alpha}^{o'} + (1-\eta)B_0 g_{0\alpha}^{c'}]$$

$$+ \left[(1-\eta)B_0\left[\alpha\Omega_0+\frac{\iota}{T_2}\right] - \iota(1-\eta)\left[\frac{1+(1-\eta B_0)}{\tau} - \frac{(1-\eta)B_0}{\tau_{op}}\right]\right]g_{0\alpha}^{c'} = 0 .$$

(4.46)

Unfortunately the solution for $g_{0\alpha}=(1-\eta)g_{0\alpha}^c + \eta g_{0\alpha}^0$ cannot be found in a closed form and one has to resort to the approximation that fields and spin polarizations are proportional to $e^{\iota qz_0}$ with small q. The solutions for $g_{0\alpha}^c$ and $g_{0\alpha}^o$, correct to first order in q^2, can be found by neglecting terms of the order of $\eta(\beta q^2/\omega)^2$;

$$g_{0\alpha'} = (1-\eta)g_{0\alpha'}^c + \eta g_{0\alpha'}^o$$

$$= \frac{-\omega\gamma\hbar/2}{\omega + \alpha\omega_s + \iota/T + \gamma_0^B\beta q^2}h_\alpha ,$$

(4.47)

where

$$\beta = \gamma_0^B[(1-\eta)\beta^c + \eta\beta^o] ,$$

(4.48)

and $T = T_2/\gamma_0^B$. By using Eqs. (4.44) and (4.47), one gets Bloch equations corresponding to Eqs. (4.22) and (4.25):

$$\omega\mathcal{M}_\alpha + (\alpha\omega_s + \iota/T - \iota D^*\nabla_0^2)(\mathcal{M}_\alpha - \mathcal{X}h_\alpha) = 0 , \quad (4.49a)$$

or equivalently

$$\frac{\partial \mathbf{M}}{\partial t} = \gamma_0\mathbf{M}\times\mathbf{H} - \frac{\mathbf{M}-\mathbf{M}_{eq}}{T} + D^*\nabla_0^2(\mathbf{M}-\mathbf{M}_{eq}) , \quad (4.49b)$$

where $\mathbf{M}_{eq} = \mathcal{X}\mathbf{H} = \mathcal{X}(\mathbf{H}_0+\mathbf{h})$, $\mathbf{M} = \mathbf{M}_{eq}+\mathcal{M}$, $D^* = \gamma_0^B\beta/\iota$, and $\mathcal{X} = \mathcal{X}_0/\gamma_0^B$ is the susceptibility of an interacting electron gas.

All the modifications caused by CDW effects incorporated in this work, i.e., the anisotropic velocity distribution, the presence of open orbits, and the CDW Q-domain structure, are contained in Eq. (4.48). β^o depends on the Q-domain size D through Eqs. (4.39) and (4.42).

D. Transmitted signals

A standard way of finding a transmitted signal through a finite slab is to utilize the Bloch equation (4.49) with an appropriate boundary condition. From Eq. (4.49), one can see that the magnetization current $\mathbf{J}_\mathcal{M}$ is given by $-\nabla_0(\mathbf{M}-\mathbf{M}_{eq})$, or equivalently $-\nabla_0(\mathcal{M}-\mathcal{X}h)$.[5] The subscript α is dropped since only the $\alpha = -1$ component is resonant. The appropriate boundary condition in the absence of surface spin relaxation is

$$\hat{n}\cdot\mathbf{J}_\mathcal{M} = \hat{n}\cdot\nabla_0(\mathcal{M}-\mathcal{X}h) = 0 . \quad (4.50)$$

A simpler way is to solve the Bloch equation with the above boundary condition for $\mathcal{M}'$;

$$\omega\mathcal{M}' + (-\omega_s + \iota/T - \iota D\nabla_0^2)\mathcal{M}' = -\omega\mathcal{X}h . \quad (4.51)$$

The boundary condition (4.50) becomes

$$\hat{n}\cdot\nabla_Q\mathcal{M}'=0 \ . \tag{4.52}$$

When fields and magnetization are assumed to depend only on z_0, Eq. (4.51) becomes

$$\frac{d^2}{dz_0^2}\mathcal{M}'+k^2\mathcal{M}'=\frac{\omega\chi}{\iota D}h \ , \tag{4.53}$$

where

$$k^2=\frac{\iota(\omega-\omega_s)T-1}{D^*T} \ , \tag{4.54}$$

and

$$\left[\frac{d\mathcal{M}'}{dz_0}\right]_{z_0=\pm L/2}=0 \ . \tag{4.55}$$

The solution for $\mathcal{M}$ can be readily found to be

$$\mathcal{M}=\chi h+\frac{\omega\chi}{\iota D^*}\frac{1}{k\sin^2 W}\left\{\cos\left[k\left[z-\frac{L}{2}\right]\right]\int_{-L/2}^z dz'\cos\left[k\left[\frac{L}{2}+z'\right]\right]h(z')\right.$$

$$\left.+\cos\left[k\left[z+\frac{L}{2}\right]\right]\int_z^{L/2}dz'\cos\left[k\left[\frac{L}{2}-z'\right]\right]h(z')\right\} \ , \tag{4.56}$$

where $W=kL/2$. Equation (4.56) was obtained by Walker,[28] and the second term describes the spin-wave excitation. The transmitted signal can be found to be proportional to the magnetization just inside the surface at $z=L/2$,[5,28]

$$H(L_+/2)=cZ_0M(L_-/2) \ , \tag{4.57}$$

where Z_0 is the surface impedance for spinless electrons.

$$H_T\propto\frac{\iota}{[(\omega-\omega_s)T_2+\iota]}\left|\frac{2W}{\sin 2W}\right| \ , \tag{4.58}$$

which was first obtained by Platzman and Wolff using a Green's-function technique.[5]

V. COMPARISON WITH THE PLATZMAN-WOLFF THEORY AND EXPERIMENTAL DATA

Although the Wilson-Fredkin theory[6] was shown to explain experimental data better than the Platzman-Wolff theory, the two theories are equally satisfactory[11] if one neglects B_n and $n\geq 2$ and anomalous experimental features reproduced in Fig. 7. Hence we will compare CDW theory only with Platzman-Wolff theory for potassium, for which the direction and magnitude of Q were recently determined.[16] In Fig. 5, comparisons are made for two different geometries with only open-orbit effects included, assuming that the direction of G_{110} is perpendicular to the surface of the sample (which is indicated by optical experiments[24]), that the azimuthal angle of H_0 about $\hat{Q}'$ is zero, defined in Fig. 4 with $\hat{Q}'$ parallel to $\hat{z}$, and that the CDW domain size is 0.001 cm. Q is (0.995,0.975,0.015) in units of $2\pi/a$ and the angle between Q and G_{110} is 0.85°. $Q'=(0.005,0.025,-0.015)$ in units of $2\pi/a$ and the angle between Q' and G_{110} is 44.18°. All modifications caused by CDW effects are contained in the effective diffusion constant D^* in Eq. (4.49), or equivalently β in Eq. (4.48) through Eqs. (4.37), (4.39), and (4.42). Since the inclusion of distortion effects does not change the following results qualitatively, all comparisons with experimental data will be made with only open-orbit effects included. The positions of the side bands agree very well, while the different signal amplitudes and widths can be made to agree with experiment by adjusting the relaxation times τ and T_2. T_2 deter-
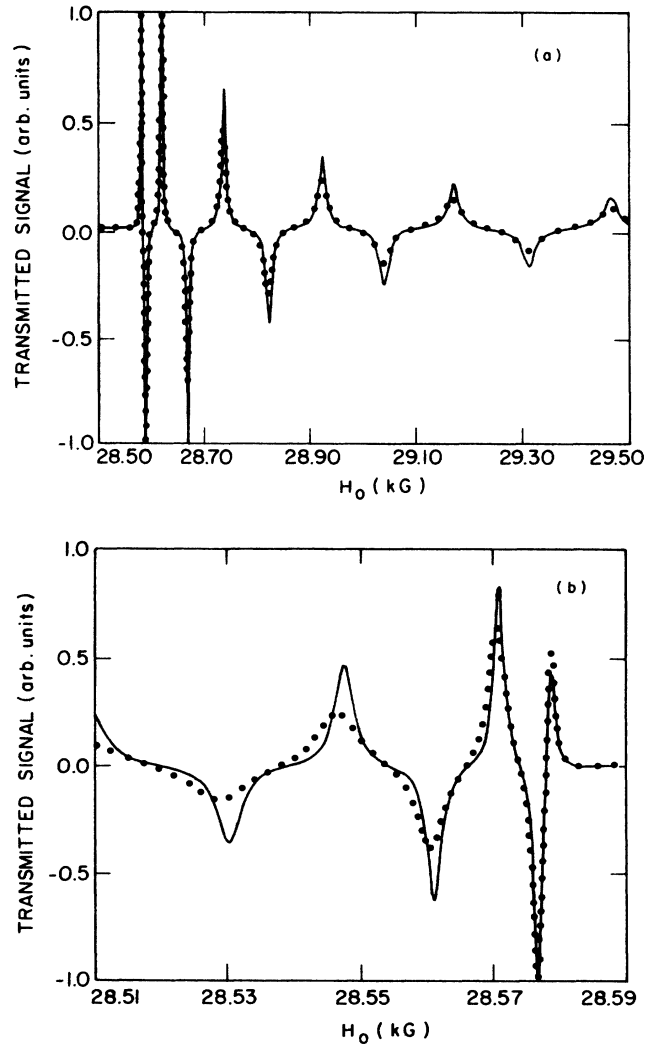

FIG. 5. Comparison between the CDW theory and PW theory: the dotted curve for the CDW theory with only open-orbit effects included; the solid curve for the PW theory. No attempt was made to make the amplitudes and widths agree with experimental data, by readjusting τ and T_2 (for the CDW case). (a) For the field-perpendicular geometry. (b) For the field-parallel geometry.

mines the decay rate of the amplitudes of the side band peaks, and τ determines their widths. Our theory does not explain the variation of the width of the main CESR peak versus Δ, and τ and T_2 would be adjusted following the procedure taken by Mace, Dunifer, and Sambles.[11] For the PW theory, $B_0 = -0.292$ and $B_1 = -0.073$ were used,[11] whereas for the CDW theory it was found that $B_0 = -0.252 \pm 0.003$ and $\eta = 0.048 \pm 0.015$ with the open-orbit effect included and $B_0 = -0.221 \pm 0.002$ and $\eta = 0.042 \pm 0.013$ with both the open-orbit effect and the distortion effect included. "$\pm$" indicates the upper and lower bounds for the range of azimuthal angle of $\mathbf{H}_0$ about $\hat{\mathbf{Q}}$, defined in Fig. 4 with $\hat{\mathbf{Q}}$ parallel to $\hat{\mathbf{q}}$. The variation of the fitting parameters B_0 and η over the azimuthal angle is shown in Fig. 6. When the Q-domain size is larger than 0.002 cm, B_0 and η vary much more rapidly and spin-wave side bands show splittings into two or more components as will be discussed later. This variation can be attributed to the fact that the magnetic field along $\mathbf{Q}'$ vanishes for some azimuthal angles and the effective diffusion constant near those angles changes rapidly. One can see that the magnitude of B_0 depends critically on the various CDW effects, and that there will be a systematic change in the positions of side band peaks as the azimuthal angle is changed for samples having large CDW domain size.

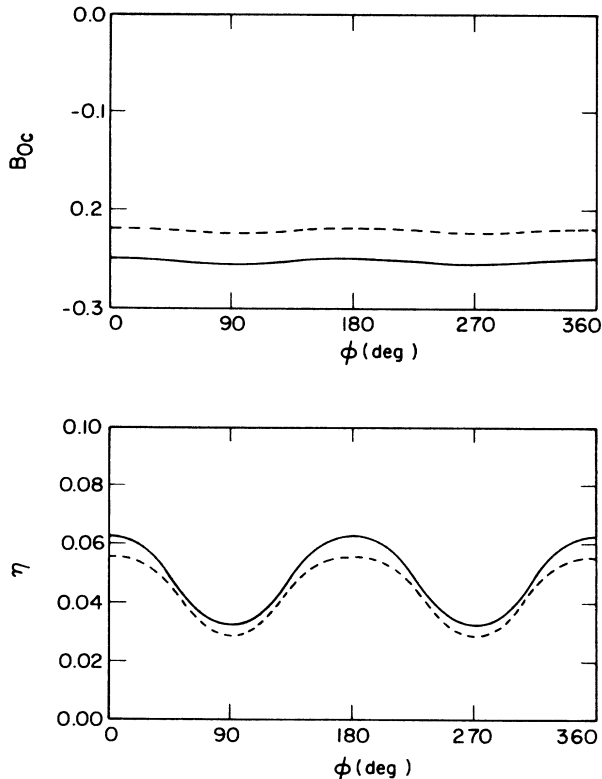Although extreme care was taken in preparing sam-

ples, it was reported[11] that even the best samples displayed some imperfections: a faint milky appearance, numerous small bubbles at the surface, and microscopic protrusions due to shallow scratches on the quartz windows. When samples showed splitting of either the main CESR or side bands, they were simply thought unacceptable and discarded. It was reported that there were extra features having the characteristic of spin-wave signals in the vicinity of the first two spin waves, reproduced in Fig. 7(a) from Fig. 14(a) of Ref. 11, and side bands sometimes split into two or more components, reproduced in Fig. 7(b) from Fig. 13(a) of Ref. 11. Figure 7(a) was obtained in Na and Fig. 7(b) was obtained in K, but these features were observed in both Na and K. The anomalous features in Fig. 7(a) were left unexplained and the splittings in Fig. 7(b) were attributed in the report to different thickness within the sample, although the variation in thickness was typically less than 1%. But we believe that unless there is a systematic, much larger difference in thickness, splitting of a side band cannot occur, since what is measured is the transmitted microwave from the whole surface of the sample. Also it was reported that the main CESR peak sometimes splits into two or more

FIG. 6. Variation of fitting parameters as a function of the azimuthal angle between $\mathbf{Q}$ and $\mathbf{H}_0$ for domain size $D = 0.001$ cm. The solid curve obtains when only open-orbit effects are included, and the dashed curve applies when the Fermi surface distortion is also included.
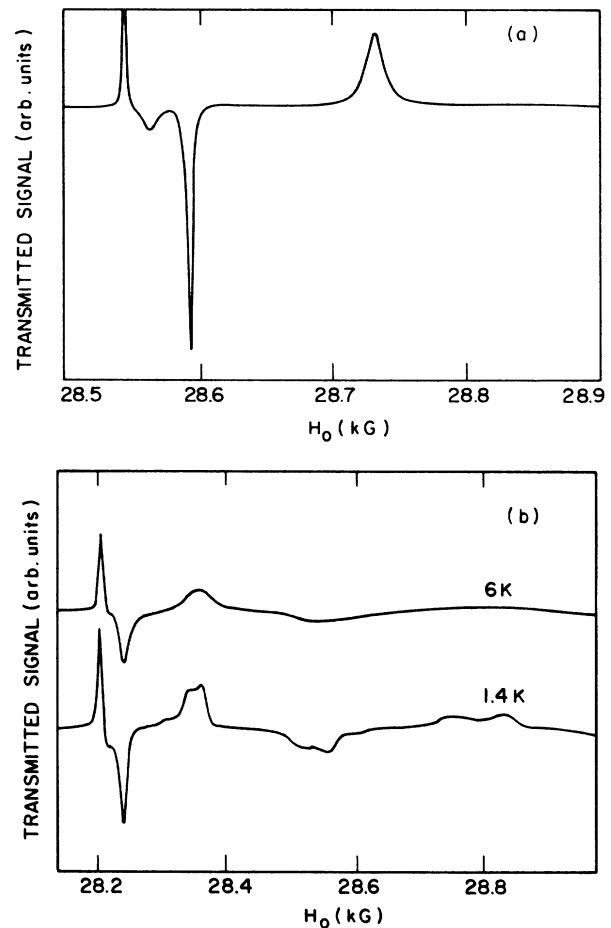

FIG. 7. Anomalous experimental data. (a) Extra feature between the main CESR and the first spin wave in Na. (b) Splitting of side band peaks in K.
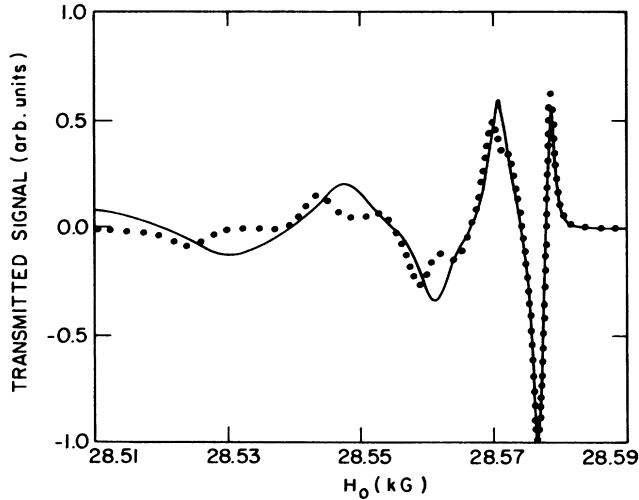
FIG. 8. Theoretical splitting of spin-wave signals for the field-parallel geometry. $\tau = 2.6 \times 10^{-10}$ sec; $T_2 = 5.7 \times 10^{-8}$ sec; $\theta^{\text{open}} = 44.18°$; domain size $D = 0.001$ cm for the solid curve and $D = 0.01$ cm for the dotted curve.

peaks. This was attributed to inhomogeneity of the static magnetic field, since the signal changes when the inhomogeneity is adjusted. But it is not clear how a small inhomogeneity of 0.6 G, possible in a superconducting magnet, can cause the CESR signal to split into two or more peaks. This phenomena was explained by Overhauser and de Graaf[10] using CDW theory. It is natural for the CESR signal to change with field inhomogeneity since different CDW domains have different locations in the solenoid, and the change does not necessarily indicate that the splitting is due to the field inhomogeneity.

For the field-parallel geometry, $\Delta = 90°$, the domain structure is assumed to be such that any azimuthal angle of the open-orbit direction $\hat{Q}'$ about the normal to the surface, defined in Fig. 4 with $\hat{Q}'$ parallel to $\hat{z}$, is equally probable and the average of the transmitted signal H_t is taken over the azimuthal angle. In Fig. 8, the splitting of side bands appears naturally for samples with large Q-domain size whereas the splitting does not appear for samples with small domain size. For the field-perpendicular geometry, $\Delta = 0°$, different orientations of CDW wave vector Q which are crystallographically equivalent are included. Other possible open-orbit directions are 17.02°, 61.44°, 76.17°, 103.83° (equivalent to 76.17°), and 118.56° (equivalent to 61.44°). The directions 61.44° and 76.17° were chosen since they result in larger splittings, and were included to obtain Fig. 9. In Fig. 9, the splitting of side bands appears naturally for samples with large domain size. These splittings are due to extra spin waves from different CDW domains. Positions of these extra signals depend crucially on the CDW wave vector Q, and the extra features observed for Na in Fig. 7(a) could be interpreted as extra spin-wave signals from different CDW domains, similar to Fig. 9(a). These anomalous features will become less prominent as the temperature of the samples is raised, as observed, since
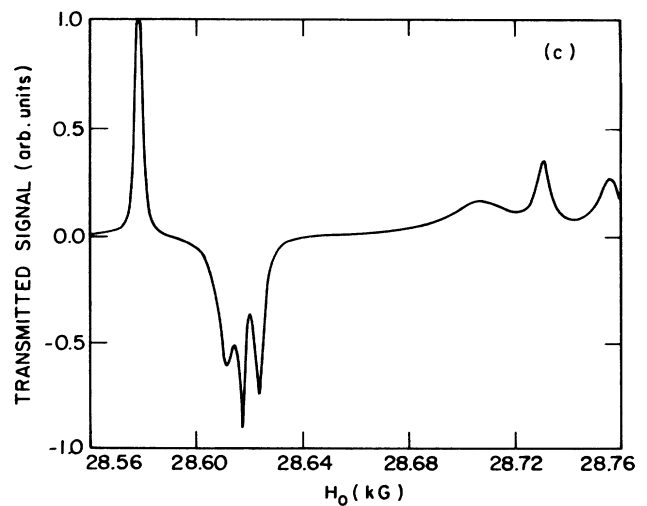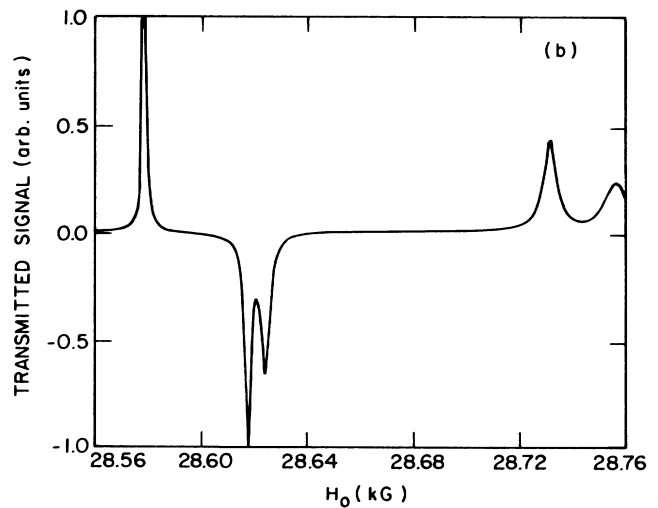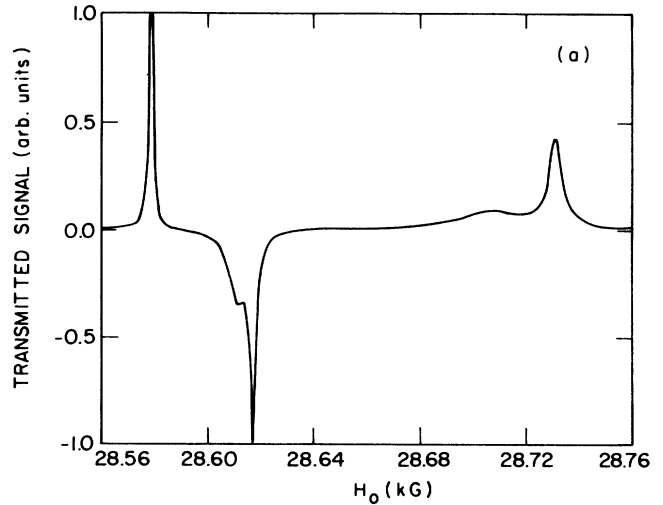

FIG. 9. Theoretical splitting of spin-wave signals for the field-perpendicular geometry. $\tau = 5.2 \times 10^{-10}$ sec, $T_2 = 5.7 \times 10^{-8}$ sec, $D = 0.02$ cm. (a) $\theta_1^{\text{open}} = 44.18°$, $\theta_2^{\text{open}} = 61.44°$ (0.5 + 0.5). (b) $\theta_1^{\text{open}} = 44.18°$, $\theta_2^{\text{open}} = 76.17°$ (0.5 + 0.5). (c) $\theta_1^{\text{open}} = 44.18°$, $\theta_2^{\text{open}} = 61.44°$, $\theta_3^{\text{open}} = 76.17°$ (0.2 + 0.5 + 0.3).

individual components will become broader (as the momentum relaxation time decreases) and will eventually merge into smooth peaks. Lattice imperfections mentioned above are expected to contribute to the formation of CDW domains having Q tilted with respect to the normal to the sample surface. Hence elimination of small pockets of argon gas between the metal and quartz window will tend to eliminate such splitting, as observed. Also the adjustments on the homogeneity control (of the static magnetic field) could make anomalous features weaker, since different domains would then be probed with magnetic fields of different strengths.

CDW domain structure is rather sensitive to the past history of a sample and similarly prepared samples can have different CDW domain structure. This explains why spin-wave signals were split for some samples and not for others and why no systematic behavior of the above-mentioned anomalous features was observed for different samples with different thicknesses. As discussed above, the observed anomalous data can be interpreted without recourse to field inhomogeneity or variation in the sample thickness. We suggest that splitting of spin-wave signals results from CDW Q-domain structure.

VI. CONCLUSION

We have shown that the occurrence of open orbits and distortion of the Fermi surface (caused by a CDW state) modify significantly an electron's motion and influence thereby paramagnetic spin-wave signals. The revised values of the Landau parameter B_0 and the fraction of electrons in open orbits η for potassium, with CDW-domain size $D=0.001$ cm, are found to be $B_0 = -0.252(\pm 0.008)$ and $\eta = 0.048(\pm 0.015)$ when only open-orbit effects are included. $B_0 = -0.221(\pm 0.002)$ and $\eta = 0.042(\pm 0.013)$ when Fermi-surface distortion effects are also included. We also observed that the splitting of spin-wave signals into two or more components can be naturally explained within the framework of CDW theory.

ACKNOWLEDGMENT

[1]T. W. Griswold, A. F. Kip, and C. Kittel, Phys. Rev. Lett. **88**, 951 (1952).

[2]F. J. Dyson, Phys. Rev. **98**, 349 (1955).

[3]M. Lampe and P. M. Platzman, Phys. Rev. **150**, 340 (1966).

[4]V. P. Silin, Zh. Eksp. Teor. Fiz. **33**, 1227 (1957) [Sov. Phys.—JETP **6**, 945 (1958)]; **35**, 1243 (1958) [**8**, 870 (1959)].

[5]P. M. Platzman and P. A. Wolff, Phys. Rev. Lett. **18**, 280 (1967); *Waves and Interactions in Solid State Plasmas* (Academic, New York, 1973).

[6]A. R. Wilson and D. R. Fredkin, Phys. Rev. B **2**, 4656 (1970).

[7]M. B. Walker, Phys. Rev. B **3**, 30 (1971).

[8]H. Mayer and M. H. El Naby, Z. Phys. **174**, 269 (1963); P. G. Coulter and W. R. Datars, Phys. Rev. Lett. **45**, 1021 (1980); for a review of these phenomena, see A. W. Overhauser, in *Highlights of Condensed-Matter Theory*, Proceedings of the International School of Physics "Enrico Fermi," Course, LXXXIX Varenna on Lake Como, 1983 edited by F. Bassani, F. Fumi, and M. P. Tosi (North-Holland, Amsterdam, 1985).

[9]W. M. Walsch, Jr., L. W. Rupp, Jr., and P. H. Schmidt, Phys. Rev. **142**, 414 (1966).

[10]A. W. Overhauser and A. M. de Graaf, Phys. Rev. **168**, 763 (1968).

[11]D. A. H. Mace, G. L. Dunifer and J. R. Sambles, J. Phys. F **14**, 2105 (1984).

[12]A. W. Overhauser, Phys. Rev. **128**, 1437 (1962); **167**, 691 (1968).

[13]C. Kittel, in *Introduction to Solid State Physics*, 4th ed. (Wiley, New York, 1971).

[14]W. R. Marquardt and J. Trivisonno, J. Phys. Chem. Solids **26**, 273 (1965).

[15]P. A. Smith and C. S. Smith, J. Phys. Chem. Solids **26**, 279 (1965).

[16]T. M. Giebultowicz, A. W. Overhauser, and S. A. Werner, Phys. Rev. Lett. **56**, 1485 (1986). Apparently conflicting data: L. Pintschovius, O. Blaschko, G. Krexner, M. de Podesta, and R. Currat, Phys. Rev. B **35**, 9930 (1987), can be interpreted by differing CDW domain structure in different samples.

[17]A. W. Overhauser, Phys. Rev. Lett. **13**, 190 (1964).

[18]F. E. Fragachan and A. W. Overhauser, Phys. Rev. B **29**, 2912 (1984).

[19]A. W. Overhauser, Phys. Rev. B **34**, 7632 (1986).

[20]L. D. Landau, Zh. Eksp. Teor. Fiz. **30**, 1058 (1956) [Sov. Phys.—JETP **3**, 920 (2957)]; **32**, 59 (1957) [**5**, 101 (1957)]; **35**, 97 (1958) [**8**, 70 (1959)].

[21]D. Pines and P. Nozières, *The Theory of Quantum Liquid* (Benjamin, New York, 1966).

[22]E. M. Lifshitz and L. P. Pitaevskii, *Statistical Physics* (Pergamon, New York, 1980), Vol. 2.

[23]V. P. Silin, Zh. Eksp. Teor. Fiz. **33**, 495 (1957) [Sov. Phys.—JETP **6**, 387 (1958)].

[24]A. W. Overhauser and N. R. Burtler, Phys. Rev. B **14**, 3371 (1976); G. F. Giuliani and A. W. Overhauser, Phys. Rev. B **20**, 1328 (1979).

[25]H. C. Torrey, Phys. Rev. **104**, 563 (1956).

[26]J. I. Kaplan, Phys. Rev. **115**, 575 (1959).

[27]M. Huberman and A. W. Overhauser, Phys. Rev. Lett. **47**, 682 (1981).

[28]M. B. Walker, Can. J. Phys. **48**, 111 (1970).